Loss of *Nupr1* promotes engraftment by tuning the dormancy threshold of hematopoietic stem cell repository via regulating p53-checkpoint pathway

Tongjie Wang[1,2,3,7], Chengxiang Xia[1,2,3,4,7], Hui Cheng[5], Qitong Weng[1], Kaitao Wang[6], Yong Dong[1], Sha Hao[5], Fang Dong[5], Xiaofei Liu[1], Lijuan Liu[1], Yang Geng[1], Yuxian Guan[1], Juan Du[1], Tao Cheng[5*], and Jinyong Wang[1,2,3,4*]

[1]State Key Laboratory of Experimental Hematology, Guangzhou Institutes of Biomedicine and Health, Chinese Academy of Sciences, Guangzhou, China;

[2]Guangzhou Regenerative Medicine and Health-Guangdong Laboratory (GRMH-GDL), Guangzhou, China;

[3]Guangdong Provincial Key Laboratory of Stem cell and Regenerative Medicine, Guangzhou Institutes of Biomedicine and Health, Chinese Academy of Sciences, Guangzhou, China;

[4]University of Chinese Academy of Sciences, Beijing, China;

[5]State Key Laboratory of Experimental Hematology & National Clinical Research Center for Blood Diseases, Institute of Hematology & Blood Diseases Hospital, Chinese Academy of Medical Sciences & Peking Union Medical College, Tianjin, China

[6]Joint School of Life Sciences, Guangzhou Institutes of Biomedicine and Health, Guangzhou Medical University, Guangzhou, China;

[7]Equal contributors

Running head: *Nupr1* regulates the dormancy threshold of HSCs

Correspondences: wang_jinyong@gibh.ac.cn (J.W.), chengtao@ihcams.ac.cn (T.C.)

Acknowledgments

This work was supported by grants from Strategic Priority Research Program of the Chinese Academy of Sciences (XDA16010601), Key Research & Development Program of Guangzhou Regenerative Medicine and Health Guangdong Laboratory (2018GZR110104006), CAS Key Research Program of Frontier Sciences (QYZDB-SSW-SM057), Healthcare Cooperative Innovation Key program of Guangzhou Science and Technology Planning Project (20183040017), the Major Research and Development Project of China (2019YFA0110203, 2019YFA0110202), Science and Technology Planning Project of Guangdong Province (2017B030314056), and the grants from the National Natural Science Foundation of China (31600948).

Abstract

Hematopoietic stem cells (HSCs) are dominantly quiescent under homeostasis, which is a key mechanism of maintaining the HSC pool for life-long hematopoiesis. Dormant HSCs poise to be immediately activated on urgent conditions and can return to dormancy after regaining homeostasis. To date, the molecular networks of regulating the threshold of HSC dormancy, if exist, remain largely unknown. Here, we unveiled that deletion of *Nupr1*, a gene preferentially expressed in HSCs, activated the dormant HSCs under homeostatic status, which conferred engraftment competitive advantage on HSCs without compromising their stemness and multi-lineage differentiation abilities in serial transplantation settings. Following an expansion protocol, the *Nupr1*$^{-/-}$ HSCs proliferate more robustly than their wild type counterparts *in vitro*. *Nupr1* inhibits the expression of p53 via an unknown mechanism and the rescue of which offsets the engraftment advantage. Our data unveil the *de novo* role of *Nupr1* as an HSC dormancy-regulator, which provides insights into accelerating the engraftment efficacy of HSC transplantation by targeting the HSC dormancy-controlling network.

Introduction

Hematopoietic stem cells (HSCs), the seeds of adult blood system, generate all the blood lineages via hierarchical hematopoiesis. Under steady-state, the majority of HSCs are maintained in dormancy to reserve the HSC pool for life-long hematopoiesis[1]. However, the dormant HSCs can be rapidly activated for stress hematopoiesis on emergency conditions, such as excessive blood loss, radiation injury, and chemotherapy damage[2]. Mounting evidence point to the existence of intrinsic molecular machinery of regulating HSC dormancy. In haploinsufficient *Gata2*$^{+/-}$ mice, HSCs show mildly increase of quiescent cells on homeostasis condition[3]. JunB inactivation deregulates the cell-cycle machinery and reduces quiescent HSCs[4]. *Hif-1α*-deficient HSCs also show decreased dormant HSCs[5]. CDK6, a protein not expressed in long-term HSCs but short-term HSCs, regulates the quiescence exit in human hematopoietic stem cells, and overexpression of which promotes engraftment[6]. To date, the underlying signaling regulatory network of HSC quiescence remains largely unknown.

NUPR1 (Nuclear protein transcription regulator 1) is a member of the high-mobility group of proteins, which was first discovered in the rat pancreas during the acute phase of pancreatitis and was initially called p8[7]. The same gene was discovered in breast cancer and was named as Com1[8]. NUPR1 demonstrates various roles involving apoptosis, stress response, and cancer progression, which depends on distinct cellular context. In certain cancers, such as breast cancer, NUPR1 inhibits tumor cell apoptosis, induces tumor establishment and progression[9-12]. On the contrary, in

prostate cancer and pancreatic cancer, NUPR1 shows tumor-growth inhibitory effect[13, 14]. Accumulated studies reveal that NUPR1 is a stress-induced protein: interference of NUPR1 can upregulate the sensitivity astrocytes to oxidative stress[15]; loss of it can promote resistance of fibroblasts to adriamycin-induced apoptosis[16]; NUPR1 mediates cannabinoid-induced apoptosis of tumor cells[17]; overexpression of *NUPR1* can negatively regulate MSL1-dependent HAT activity in Hela cells, which induces chromatin remodeling and relaxation allowing access to DNA of the repair machinery[18]. Nonetheless, the potential roles of *Nupr1*, which is preferentially expressed in HSC among the HSPC, in hematopoiesis remain elusive.

NUPR1 interacts with p53 to regulate cell cycle and apoptosis responding to stress in breast epithelial cells[16, 19]. p53 plays several roles in homeostasis, proliferation, stress, apoptosis, and aging of hematopoietic cells[20-24]. Deletion of p53 upregulates HSC self-renewal but impairs their repopulating ability and leads to tumors[25]. Hyperactive expression of p53 in HSCs decreased the HSC pool size, reduced engraftment and deep quiescence[26-28]. These reports support the essential check-point role of p53 in regulating HSC fate. Nonetheless, it is unknown whether NUPR1 and p53 coordinately regulate the quiescence of HSCs.

Here, we used a *Nupr1* conditional knockout model to investigate the consequences of loss of function of *Nupr1* in HSC context. *Nupr1*-deletion in HSCs led to their dormancy withdrawal under homeostasis. In a competitive repopulation setting, *Nupr1*-deleted HSCs robustly proliferated and showed dominant engraftment over wild type counterparts. Besides, *Nupr1*-deleted HSCs expanded abundantly and

97 preserved their stemness in vitro in comparison with wild type HSCs. The rescued
98 expression of p53 by *Mdm2*$^{+/-}$ offset the effects introduced by loss of *Nupr1* in HSCs.
99 Our studies reveal the *de novo* role and signaling mechanism of *Nupr1* in regulating
100 the quiescence of HSCs.

101 **Results**

102 **Loss of *Nupr1* accelerates the turn-over rates of HSCs under homeostasis**

103 A majority of long-term HSCs are quiescent under homeostasis, which is a key
104 mechanism for maintaining the HSC pool for life-long steady hematopoiesis. We
105 hypothesize that among those genes, preferentially expressed in HSCs but
106 immediately down regulated in MPPs, might form an intrinsic regulatory network for
107 maintaining the HSC dormancy. To test our hypothesis, we explored such factor
108 candidates by RNA-Seq analysis of the sorted HSCs (Hematopoietic stem cells, Lin$^-$
109 CD48$^-$ Sca1$^+$ c-kit$^+$ CD150$^+$) and MPPs (Multipotent stem cells, Lin$^-$ CD48$^-$ Sca1$^+$
110 c-kit$^+$ CD150$^-$). Differential expression gene analysis showed a pattern of
111 HSC-preferential transcription factors, including *Rorc*, *Hoxb5*, *Rarb*, *Gfi1b*, *Mllt3*,
112 and *Nupr1*. By literature search, we found that most of the candidate genes were
113 reportedly not involved in regulating HSC homeostasis. Thus, we focus on the *Nupr1*
114 gene, the role of which in hematopoiesis has not been reported. The expression of
115 *Nupr1* in HSCs is significantly higher (> 25-fold, p = 0.002) than MPPs (Figure 1A,
116 left). Real-Time PCR further confirmed the same expression pattern (p <0.001),
117 implicating an unknown role of *Nupr1* in HSCs (Figure 1A, right).

118 To study whether *Nupr1* has any potential impact on the hematopoiesis of HSCs, we

119 constructed the *Nupr1* conditional knockout mice by introducing two loxp elements
120 flanking the exon 1 and 2 of *Nupr1* locus using a C57BL/6 background mESC line
121 (Figure 1B). The generated *Nupr1*$^{fl/fl}$ mice were further crossed to Vav-Cre mice to
122 generate *Nupr1*$^{fl/fl}$; Vav-Cre compound mice (*Nupr1*$^{-/-}$ mice). Adult *Nupr1*$^{-/-}$ mice
123 (8-10-week-old) had a normal percentage of blood lineage cells in peripheral blood,
124 including CD11b^{+} myeloid, CD19^{+} B, and CD3^{+} T lineage cells (Supplementary Fig
125 1). We further investigated the potential alterations of HSC hemostasis in the absence
126 of *Nupr1*. Flow cytometry analysis demonstrated that *Nupr1*$^{-/-}$ HSC pool was
127 comparable to wild type counterparts in terms of ratios and absolute numbers
128 (Supplementary Fig 2). Subsequently, we examined the cell cycle status of *Nupr1*$^{-/-}$
129 HSCs using the proliferation marker Ki-67 and DAPI staining and found that the ratio
130 of *Nupr1*$^{-/-}$ HSCs in G0-status was reduced significantly ($p = 0.009$). Compared with
131 those of WT HSCs (median value: *Nupr1*$^{-/-}$ HSCs =68.1%, WT HSCs = 81.2%), more
132 *Nupr1*$^{-/-}$ HSCs entered G1-S-S2 and M phase (Figure 1C, D). To further confirmed
133 this novel phenotype, we performed BrdU incorporation assay, which is
134 conventionally used for assessing the turn-over rates of blood cells *in vivo*[29]. The
135 8-week-old *Nupr1*$^{-/-}$ mice and littermates were injected intraperitoneally with 1mg
136 BrdU on day 0, followed by administration of BrdU via water feeding (0.8 mg/ml) for
137 up to 5 days (Figure 1E). After three days of BrdU labeling, ~50% of *Nupr1*$^{-/-}$ HSCs
138 became BrdU^{+} compared with ~35% of WT HSCs. Kinetic analysis with BrdU
139 incorporation from day 3 to day 5 revealed that *Nupr1*$^{-/-}$ HSCs contained a 1.5-fold
140 higher BrdU^{+} population over WT HSCs (Figure 1F, G). Collectively, these data

indicate that the *Nupr1*-deletion drives HSCs entering cell cycle and accelerates their turn-over rates on homeostasis.

$Nupr1^{-/-}$ HSCs show repopulating advantage without compromising multi-lineage differentiation capacity

To confirm whether $Nupr1^{-/-}$ HSCs have repopulating advantage or disadvantage in *vivo*, we performed typical HSC-competitive repopulation assay. Two hundred and fifty thousand whole bone marrow nucleated cells (BMNCs) from $Nupr1^{-/-}$ mice (CD45.2) were transplanted into lethally irradiated recipients (CD45.1) along with equivalent WT (CD45.1) competitors. Sixteen weeks later, one million BMNCs of the primary recipients were transplanted into lethally irradiated recipients for assessing long-term engraftment (Figure 2A). We observed that donor $Nupr1^{-/-}$ cells took about 60%-70% in the primary recipients. $Nupr1^{-/-}$ cells gradually dominated in peripheral blood of recipients over time after transplantation (Figure 2B). In the chimerism, ~70% of myeloid cells and B lymphocytes were $Nupr1^{-/-}$ donor-derived cells, while ~60% of T lymphocytes were CD45.1 competitive cells (Figure 2C). To further explore whether $Nupr1^{-/-}$ HSCs dominate in chimerism, we sacrificed the chimerism and analyzed the HSCs 16 weeks after transplantation. Compared with the competitive HSCs, the proportion and absolute number of $Nupr1^{-/-}$ HSCs were significantly more (~3 folds) than the $CD45.1^{+}$ HSC competitors in primary recipients (Figure 2D, E). Previous research reported that HSCs proliferated rapidly at the expense of their long-term repopulating ability[30-34]. Interestingly, consistent with the dominating trend in primary transplantation, $Nupr1^{-/-}$ cells continuously dominated in

163 secondary recipients (Figure 3A). *Nupr1*$^{-/-}$ HSCs occupied up to 90% of the total
164 HSCs in the bone marrow (BM) of secondary recipients (Figure 3B, C). In aggregate,
165 these results indicate that the deletion of *Nupr1* promotes the repopulating ability of
166 HSCs without impairing their long-term engraftment ability.

167 **_Nupr1_-deleted HSCs expand robustly _in vitro_**

168 We next examined whether the deletion of *Nupr1* could enhance HSC expansion *in*
169 *vitro*. Fifty HSCs sorted from WT and *Nupr1*$^{-/-}$ mice were cultured *in vitro* for 10 days
170 as previously described[35] (Figure 4A). After 10-day-culture, the wild type input cells
171 achieved a yield of more than 2×10^4 cells, while *Nupr1*$^{-/-}$ HSCs produced
172 approximately 5×10^4 total cells ($p < 0.001$, Figure 4B). The colonies derived from
173 *Nupr1*$^{-/-}$ HSCs were much larger than WT HSCs (Figure 4C). Furthermore, we
174 analyzed the phenotypic HSC populations in the expanded cells and found that the
175 absolute number of phenotypic HSC in individual *Nupr1*$^{-/-}$ colonies were 3 times more
176 than WT HSCs ($p=0.005$, Figure 4D, E). To determine whether the quantitative
177 expansion of phenotypic HSC contains net proliferation of functional HSCs, we
178 performed competitive repopulating unit (CRU) assays[36], using the serial doses of
179 limiting dilutions of the in vitro expanded cells. The WT HSC frequency in the
180 10-day expanded cells is 1 in 326 cells, which is equivalent to 62 functional HSCs.
181 While the *Nupr1*$^{-/-}$ HSC frequency in the 10-day expanded cells is 1 in 251 cells
182 (Figure 4F)[37], which is equivalent to 200 functional HSCs. Therefore, the deletion of
183 *Nupr1* induced around three-fold expansion in functional HSC number over the WT
184 HSCs. Deletion of *Nupr1* enhances the expansion ability of HSCs *in vitro*.

Reversion of p53 expression offsets the competitiveness of *Nupr1*$^{-/-}$ HSCs

To further investigated the underlying molecular mechanisms of *Nupr1* in regulating HSCs, we performed RNA-Seq analysis of *Nupr1*$^{-/-}$ HSCs from 8-week-old *Nupr1*$^{-/-}$ mice. Gene set enrichment analysis (GSEA) illustrated that p53 pathways feedback loops-related genes, including *Trp53*, *Ccng1*, *Ctnnb1*, *Pten*, and *Pik3c2b*, were enriched in WT HSCs (Figure 5A). p53 pathway regulates a series of target genes involving cell cycle arrest, apoptosis, senescence, DNA repair, and metabolism[38]. Interestingly, the expression of p53 was significantly ($p < 0.001$) reduced to 1/3 of control in *Nupr1*$^{-/-}$ HSCs (Figure 5B). Therefore, we hypothesized that down-regulation of p53 in *Nupr1*$^{-/-}$ HSCs might account for the competitive advantage of the HSCs. MDM2 is a ubiquitin ligase E3 for p53, which is a key repressive regulator of p53 signaling[39]. *Mdm2* deficient mice showed active p53 levels, which is an ideal substitute model of up-regulating p53 since direct overexpressing p53 leading to cell death and blood malignancies in mice[24, 40]. The *Nupr1*$^{-/-}$ mice were crossed to the *Mdm2*$^{+/-}$ mice to achieve up-regulation of p53 expression in *Nupr1*$^{-/-}$ HSCs. The expression level of p53 in *Nupr1*$^{-/-}$ and *Nupr1*$^{-/-}$*Mdm2*$^{+/-}$ HSC. The expression level of p53 protein in *Nupr1*$^{-/-}$*Mdm2*$^{+/-}$ HSCs is comparable with WT HSCs, which is significantly higher than *Nupr1*$^{-/-}$ HSCs when measured by indirect immunofluorescence assay (Figure 5C, D). Next, we examined the phenotypic HSC of the *Nupr1*$^{-/-}$*Mdm2*$^{+/-}$ mice. Flow cytometry analysis demonstrated that *Nupr1*$^{-/-}$Mdm2$^{+/-}$ HSC pool was indistinguishable with wild type and *Nupr1*$^{-/-}$ counterparts in terms of ratios and absolute numbers (Figure 6A, B). Further, we

tested the competitiveness of *Nupr1*$^{-/-}$*Mdm2*$^{+/-}$ HSCs in parallel with *Nupr1*$^{-/-}$ HSCs. Two hundred and fifty thousand whole bone marrow nucleated cells from *Nupr1*$^{-/-}$ *Mdm2*$^{+/-}$ mice (CD45.2) or *Nupr1*$^{-/-}$ mice (CD45.2) were transplanted into lethally irradiated recipients (CD45.1) along with equivalent WT (CD45.1) whole bone marrow nucleated cells. In the recipients of *Nupr1*$^{-/-}$*Mdm2*$^{+/-}$ donor cells, the contribution of *Nupr1*$^{-/-}$*Mdm2*$^{+/-}$ cells was significantly ($p < 0.001$) reduced to ~20%, which was far below the percentage of *Nupr1*$^{-/-}$ cells in recipients of *Nupr1*$^{-/-}$ donor cells (Figure 6C). Sixteen weeks after transplantation, we also analyzed the *Nupr1*$^{-/-}$*Mdm2*$^{+/-}$ HSCs in the chimerism. Surprisingly, the *Nupr1*$^{-/-}$*Mdm2*$^{+/-}$ HSCs almost disappeared in the HSC pool of the recipients, while the *Nupr1*$^{-/-}$ HSCs dominantly occupied in the HSC pool (Figure 6D, E). Altogether, the reversion of p53 expression offsets the competitiveness advantage of *Nupr1*$^{-/-}$ HSCs.

Discussion

The intrinsic networks of regulating the quiescence of HSCs are largely unknown. In this study, loss of *Nupr1* (p8), a gene preferentially expressed in long-term HSCs, tunes the dormancy threshold of HSCs on homeostasis condition without compromising their key functions in hematopoiesis. *Nupr1* coordinates with p53 to form a signaling machinery regulating HSC quiescence and turnover rate. For the first time, we unveil the *de novo* role of *Nupr1* in controlling HSC dormancy.

Nupr1$^{-/-}$ HSCs replenished faster than WT HSCs under homeostasis. However, the size of *Nupr1*$^{-/-}$ HSC pool was not altered. These data implicate that despite the existence of intrinsic machinery of controlling HSC dormancy, the scale of HSC-pool

is restricted by extrinsic bone marrow microenvironment[41]. Conventionally, molecules activating HSCs showed transiently phenotypic proliferation of HSCs but eventually led to their functional exhaustion and even tumors[30-34]. Interestingly, *Nupr1* signaling seemingly plays a unique role in regulating HSC dormancy and turnover rates, as deletion of *Nupr1* maintains the hematopoiesis features of HSCs. Consistently, enforced CDK6 expression in HSCs confers competitive advantage without impairing their stemness and multi-lineage potential[6]. These evidence supports the concept that targeting the intrinsic machinery of balancing HSC dormancy threshold might safely promoting engraftment.

Loss of *Nupr1* in HSCs resulted in engraftment advantage. Under the transplantation stress settings, the HSC niche occupied by WT HSCs was ablated, providing niche vacuum for donor *Nupr1*$^{-/-}$ HSC entrance. The dominance of *Nupr1*$^{-/-}$ HSCs is a consequence of fast turnover rate of these cells over WT counterparts. In the previous research, loss of Dnmt3a also leads to clonal dominance of HSCs, however, accompanied with hematopoiesis failure due to differentiation block[42, 43]. Thus, the engraftment advantage caused by loss of *Nupr1* might have prospective translational implications for hematopoietic stem cells transplantation (HSCT), since a faster recovery of hematopoiesis in transplanted host definitely reduces infection risks in patients[44, 45].

In our models, *Nupr1* regulated hematopoietic homeostasis via targeting p53 pathway. Consistently, p53 is essential in regulating hematopoietic homeostasis[24]. Whether NUPR1 directly interacts with p53 in HSC context remain unknown, as currently

antibodies suitable for protein-protein interaction assays are not available. NUPR1 and p53 directly interacted in human breast epithelial cells[19]. Knocking out p53 in HSCs can promote HSC expansion, but directly targeting p53 caused HSC apoptosis and tumorigenesis[46]. Thus, *Nupr1* might behave as an upstream regulator of p53 signaling and uniquely regulate cell dormancy in HSC context.

In conclusion, loss of *Nupr1* in HSCs promotes engraftment by tuning the dormancy threshold of HSCs via regulating p53 check-point pathway. Our study unveils the prospect of shortening the engraftment time of HSCT by targeting the intrinsic machinery of controlling HSC dormancy.

Materials and Methods

Mice

Animals were housed in the animal facility of the Guangzhou Institutes of Biomedicine and Health (GIBH). *Nupr1*$^{fl/fl}$ mice were constructed by Beijing Biocytogen Co., Ltd. CD45.1, Vav-cre, *Mdm2*$^{+/-}$ mice were purchased from the Jackson laboratory. All the mouse lines were maintained on a pure C57BL/6 genetic background. All experiments were conducted in accordance with experimental protocols approved by the Animal Ethics Committee of GIBH.

Flow cytometry analysis

For HSC and MPP staining, total BM cells were stained with antibodies against CD2/CD3/CD4/CD8/CD11b/Gr-1/B220/Ter119/CD48-FITC, c-Kit-APC-eFluor® 780, Sca1-Percp-cy5.5, and CD150-PE-cy7. Cells were analyzed by LSR Fortessa (BD Bioscience). For lineage analysis of peripheral blood, the white blood cells were

stained with antibodies of anti-CD45.1-FITC, anti-CD45.2-percp-cy5.5, anti-CD90.2-APC, anti-CD19-PE, anti-CD11b-PE-cy7, anti-Gr-1-APC-eFlour® 780.

HSC cell cycle analysis

We first labeled the HSCs with (CD2, CD3, CD4, CD8, Ter119, B220, Gr1, CD48)-FITC, Sca1-Percp-cy5.5, c-kit-PE-cy7, and CD150-PE. Then the cells were fixed using 4% PFA. After washing, the fixed cells were permeabilized with 0.1% saponin in PBS together with the Ki-67-APC staining for 45 minutes. Finally, the cells were resuspended in DAPI solution for staining 1 hour. The data were analyzed using Flowjo software (FlowJo).

BrdU incorporation assay

Nupr1$^{-/-}$ mice and WT littermate mice were injected with 1 mg BrdU on Day 0. Then they were fed with water containing BrdU (0.8 mg/mL). On Day 3, 4, 5 after the injection of BrdU, four mice of each group were sacrificed. The incorporation rates of BrdU were analyzed by flow cytometry according to the BD Pharmingen ™ APC BrdU Flow Kit instructions.

HSC culture

The HSC culture protocol is as described [35]. Briefly, fifty HSCs were sorted into fibronectin (Sigma)-coated 96-well U-bottom plate directly and were cultured in medium composed of F12 medium (Life Technologies), 1% insulin–transferrin–selenium–ethanolamine (ITSX; Life Technologies), 10 mM HEPES (Life Technologies), 1% penicillin/streptomycin/glutamine (P/S/G; Life Technologies), 100 ng/ml mouse TPO, 10 ng/ml mouse SCF and 0.1% PVA (P8136).

Complete medium changes were made every 2–3 days, by manually removing medium by pipetting and replacing fresh medium as indicated.

Limiting dilution assay

For limiting dilution assays[36], the 10-day cultured cells were transplanted into lethally irradiated C57BL/6-CD45.1 recipient mice, together with 2×10^5 CD45.1 bone-marrow competitor cells. Donor chimerism was analyzed as above. Limiting dilution analysis was performed using ELDA software[37], based on a 1% peripheral-blood multilineage chimerism as the threshold for positive engraftment.

Indirect Immunofluorescence Assay

Sorted HSCs were directly pipetted onto the poly-lysine coated slides (100-500 cells in 5μl) and incubated at room temperature for 10 min. Upon the solution was completely dry, the cells were fixed with 4%PFA for 10 min following with 0.15%Triton X-100 permeabilization for 2 min at room temperature. To avoid non-specific antibody binding, the cells were blocked in 1% BSA/PBS for 1-2h at room temperature and then incubated with the primary p53 antibody in 1% BSA in PBS overnight at 4℃ (Abcam, ab16465). Slides were washed three times in PBS and incubated with secondary antibodies for 1h at room temperature in 1% BSA in PBS (donkey anti-mouse Alexa Fluor® 488, Abcam, ab150105). After washing the slides, the cells were incubated with DAPI solution for 10 min. Confocal analysis was performed at high resolution with a Zeiss laser scanning confocal microscope, LSM-800. The images were processed with ZEN 2012 software (blue edition).

316 **RNA-Seq and data analysis.** For HSC library preparation, HSCs
317 ($Lin^-CD48^-Sca1^+cKit^+CD150^+$) were sorted from 8-10 weeks old *Nupr1*$^{-/-}$ mice and
318 wild type mice. HSCs were sorted from four mice of each group. 1000 target cells per
319 sample were sorted into 500 μl DPBS-BSA buffer (0.5%BSA) using 1.5ml EP tube and
320 transferred into 250 μl tube to spin down with 500 g. The cDNA of sorted 1000-cell
321 aliquots were generated and amplified as described previously[47]. The qualities of the
322 amplified cDNA were examined by Q-PCR analysis of housekeeping genes (*B2m, Actb,*
323 *Gapdh, Ecf1a1*). Samples passed quality control were used for sequencing library
324 preparation by illumina Nextera XT DNA Sample Preparation Kit (FC-131-1096).
325 For data analysis, all libraries were sequenced by illumina sequencers NextSeq 500.
326 The fastq files of sequencing raw data samples were generated using illumina bcl2fastq
327 software (version: 2.16.0.10) and were uploaded to Gene Expression Omnibus public
328 database (GSE131071). Raw reads were aligned to mouse genome (mm10) by
329 HISAT2[48] (version: 2.1.0) as reported. And raw counts were calculated by
330 featureCounts of subread[49] (version 1.6.0). Differential gene expression analysis was
331 performed by DESeq2[50] (R package version: 1.18.1). Heatmaps were plotted using
332 gplots (R package, version 3.01). GSEA was performed as described[51]. The gene set
333 (p53 pathway feedback loop) for GSEA were from PANTHER pathways dataset.
334 **Quantitative real-time PCR**
335 Total RNA was extracted from ten thousand purified HSCs and MPPs with an RNeasy
336 micro kit (QIAGEN). Then, 2 ng of RNA was used for linear amplification according
337 to the manufacturer's instructions (3302–12, Ovation Pico WTA System V2, NuGEN

Technologies, Inc.). The RNA was diluted and 10ng RNA was used as the template for quantitative real-time PCR (CFX-96, Bio-Rad). The forward primer of *Nupr1* is 5'-CCCTTCCCAGCAACCTCTAA-3'and the reverse primer is 5'-AGCTTCTCTCTTGGTCCGAC-3'. Fold expression relative to the reference gene was calculated using the comparative method $2^{-\Delta\Delta Ct}$, and the values were normalized to 1 for comparison.

Bone marrow competitive repopulation assay

One day before bone marrow transplantation, adult C57BL/6 (CD45.1, 8-10 weeks old) recipient mice were irradiated with 2 doses of 4.5Gy (RS 2000, Rad Source) for a 4-hour interval. Two hundred and fifty thousand BMNCs from *Nupr1*$^{-/-}$ mice (CD45.2) and equivalent WT (CD45.1) counterparts were mixed and injected into irradiated CD45.1 recipients by the retro-orbital injection. *Mdm2*$^{+/-}$*Nupr1*$^{-/-}$ BMNCs (CD45.2) were also mixed with equivalent competitors (CD45.1) and transplanted into recipients. The transplanted mice were maintained on trimethoprim-sulfamethoxazole-treated water for 2 weeks. For secondary transplantation, BMNCs of primary competitive transplanted recipients were obtained. One million of total BMNCs were injected into irradiated CD45.1 recipients (2 doses of 4.5Gy, one day before transplantation). Donor-derived cells and hematopoietic lineages in PB were assessed monthly by flow cytometry.

Statistic analysis

The data were represented as mean ± SD. Two-tailed independent Student's t-tests were performed for comparison of two groups of data (SPSS v.23, IBM Corp.,

Armonk, NY, USA). P values of less than 0.05 were considered statistically significant (*$p < 0.05$, **$p < 0.01$, ***$p < 0.001$).

Author contributions: T.J.W. and C.X.X. performed research, analyzed data and wrote the paper; Y.D. and Q.T.W. analyzed RNA-Seq data; H.C., S.H., F.D., K.T.W., X.F.L., L.J.L., Y.G., and Y.X.G. performed experiments; J.D. and T.C. discussed the manuscript; J.Y.W. designed research, and wrote the manuscript.

References

1. Cheshier SH, Morrison SJ, Liao X, Weissman IL. In vivo proliferation and cell cycle kinetics of long-term self-renewing hematopoietic stem cells. Proc Natl Acad Sci U S A. 1999;96(6):3120-3125.

2. Wilson A, Laurenti E, Oser G, et al. Hematopoietic stem cells reversibly switch from dormancy to self-renewal during homeostasis and repair. Cell. 2008;135(6):1118-1129.

3. Rodrigues NP, Janzen V, Forkert R, et al. Haploinsufficiency of GATA-2 perturbs adult hematopoietic stem-cell homeostasis. Blood. 2005;106(2):477-484.

4. Santaguida M, Schepers K, King B, et al. JunB protects against myeloid malignancies by limiting hematopoietic stem cell proliferation and differentiation without affecting self-renewal. Cancer Cell. 2009;15(4):341-352.

5. Takubo K, Goda N, Yamada W, et al. Regulation of the HIF-1alpha level is essential for hematopoietic stem cells. Cell Stem Cell. 2010;7(3):391-402.

6. Laurenti E, Frelin C, Xie S, et al. CDK6 levels regulate quiescence exit in human hematopoietic stem cells. Cell Stem Cell. 2015;16(3):302-313.

382 7. Mallo GV, Fiedler F, Calvo EL, et al. Cloning and expression of the rat p8 cDNA, a new gene
383 activated in pancreas during the acute phase of pancreatitis, pancreatic development, and regeneration,
384 and which promotes cellular growth. J Biol Chem. 1997;272(51):32360-32369.
385 8. Ree AH, Tvermyr M, Engebraaten O, et al. Expression of a novel factor in human breast cancer
386 cells with metastatic potential. Cancer Res. 1999;59(18):4675-4680.
387 9. Ree AH, Pacheco MM, Tvermyr M, Fodstad O, Brentani MM. Expression of a novel factor, com1,
388 in early tumor progression of breast cancer. Clin Cancer Res. 2000;6(5):1778-1783.
389 10. Ito Y, Yoshida H, Motoo Y, et al. Expression and cellular localization of p8 protein in thyroid
390 neoplasms. Cancer Lett. 2003;201(2):237-244.
391 11. Mohammad HP, Seachrist DD, Quirk CC, Nilson JH. Reexpression of p8 contributes to
392 tumorigenic properties of pituitary cells and appears in a subset of prolactinomas in transgenic mice
393 that hypersecrete luteinizing hormone. Mol Endocrinol. 2004;18(10):2583-2593.
394 12. Brannon KM, Million Passe CM, White CR, Bade NA, King MW, Quirk CC. Expression of the
395 high mobility group A family member p8 is essential to maintaining tumorigenic potential by
396 promoting cell cycle dysregulation in LbetaT2 cells. Cancer Lett. 2007;254(1):146-155.
397 13. Jiang WG, Davies G, Martin TA, Kynaston H, Mason MD, Fodstad O. Com-1/p8 acts as a putative
398 tumour suppressor in prostate cancer. Int J Mol Med. 2006;18(5):981-986.
399 14. Malicet C, Lesavre N, Vasseur S, Iovanna JL. p8 inhibits the growth of human pancreatic cancer
400 cells and its expression is induced through pathways involved in growth inhibition and repressed by
401 factors promoting cell growth. Mol Cancer. 2003;2(37.
402 15. Malicet C, Giroux V, Vasseur S, Dagorn JC, Neira JL, Iovanna JL. Regulation of apoptosis by the
403 p8/prothymosin alpha complex. Proc Natl Acad Sci U S A. 2006;103(8):2671-2676.

16. Vasseur S, Hoffmeister A, Garcia-Montero A, et al. p8-deficient fibroblasts grow more rapidly and are more resistant to adriamycin-induced apoptosis. Oncogene. 2002;21(11):1685-1694.

17. Carracedo A, Lorente M, Egia A, et al. The stress-regulated protein p8 mediates cannabinoid-induced apoptosis of tumor cells. Cancer Cell. 2006;9(4):301-312.

18. Gironella M, Malicet C, Cano C, et al. p8/nupr1 regulates DNA-repair activity after double-strand gamma irradiation-induced DNA damage. J Cell Physiol. 2009;221(3):594-602.

19. Clark DW, Mitra A, Fillmore RA, et al. NUPR1 interacts with p53, transcriptionally regulates p21 and rescues breast epithelial cells from doxorubicin-induced genotoxic stress. Curr Cancer Drug Targets. 2008;8(5):421-430.

20. Dumble M, Moore L, Chambers SM, et al. The impact of altered p53 dosage on hematopoietic stem cell dynamics during aging. Blood. 2007;109(4):1736-1742.

21. Lotem J, Sachs L. Hematopoietic cells from mice deficient in wild-type p53 are more resistant to induction of apoptosis by some agents. Blood. 1993;82(4):1092-1096.

22. Shounan Y, Dolnikov A, MacKenzie KL, Miller M, Chan YY, Symonds G. Retroviral transduction of hematopoietic progenitor cells with mutant p53 promotes survival and proliferation, modifies differentiation potential and inhibits apoptosis. Leukemia. 1996;10(10):1619-1628.

23. Bondar T, Medzhitov R. p53-mediated hematopoietic stem and progenitor cell competition. Cell Stem Cell. 2010;6(4):309-322.

24. Liu Y, Elf SE, Miyata Y, et al. p53 regulates hematopoietic stem cell quiescence. Cell Stem Cell. 2009;4(1):37-48.

25. Chen J, Ellison FM, Keyvanfar K, et al. Enrichment of hematopoietic stem cells with SLAM and LSK markers for the detection of hematopoietic stem cell function in normal and Trp53 null mice. Exp

426 Hematol. 2008;36(10):1236-1243.

427 26. Wang YV, Leblanc M, Fox N, et al. Fine-tuning p53 activity through C-terminal modification
428 significantly contributes to HSC homeostasis and mouse radiosensitivity. Genes Dev.
429 2011;25(13):1426-1438.

430 27. Liu D, Ou L, Clemenson GD, Jr., et al. Puma is required for p53-induced depletion of adult stem
431 cells. Nat Cell Biol. 2010;12(10):993-998.

432 28. Yamashita M, Nitta E, Suda T. Regulation of hematopoietic stem cell integrity through p53 and its
433 related factors. Ann N Y Acad Sci. 2016;1370(1):45-54.

434 29. Kiel MJ, He S, Ashkenazi R, et al. Haematopoietic stem cells do not asymmetrically segregate
435 chromosomes or retain BrdU. Nature. 2007;449(7159):238-242.

436 30. Motoda L, Osato M, Yamashita N, et al. Runx1 protects hematopoietic stem/progenitor cells from
437 oncogenic insult. Stem Cells. 2007;25(12):2976-2986.

438 31. Miyamoto K, Araki KY, Naka K, et al. Foxo3a is essential for maintenance of the hematopoietic
439 stem cell pool. Cell Stem Cell. 2007;1(1):101-112.

440 32. Ficara F, Murphy MJ, Lin M, Cleary ML. Pbx1 regulates self-renewal of long-term hematopoietic
441 stem cells by maintaining their quiescence. Cell Stem Cell. 2008;2(5):484-496.

442 33. Tipping AJ, Pina C, Castor A, et al. High GATA-2 expression inhibits human hematopoietic stem
443 and progenitor cell function by effects on cell cycle. Blood. 2009;113(12):2661-2672.

444 34. Campbell TB, Basu S, Hangoc G, Tao W, Broxmeyer HE. Overexpression of Rheb2 enhances
445 mouse hematopoietic progenitor cell growth while impairing stem cell repopulation. Blood.
446 2009;114(16):3392-3401.

447 35. Wilkinson AC, Ishida R, Kikuchi M, et al. Long-term ex vivo haematopoietic-stem-cell expansion

allows nonconditioned transplantation. Nature. 2019;571(7763):117-121.

36. Yamamoto R, Morita Y, Ooehara J, et al. Clonal analysis unveils self-renewing lineage-restricted progenitors generated directly from hematopoietic stem cells. Cell. 2013;154(5):1112-1126.

37. Hu Y, Smyth GK. ELDA: extreme limiting dilution analysis for comparing depleted and enriched populations in stem cell and other assays. J Immunol Methods. 2009;347(1-2):70-78.

38. Li T, Kon N, Jiang L, et al. Tumor suppression in the absence of p53-mediated cell-cycle arrest, apoptosis, and senescence. Cell. 2012;149(6):1269-1283.

39. Honda R, Tanaka H, Yasuda H. Oncoprotein MDM2 is a ubiquitin ligase E3 for tumor suppressor p53. FEBS Lett. 1997;420(1):25-27.

40. Abbas HA, Maccio DR, Coskun S, et al. Mdm2 is required for survival of hematopoietic stem cells/progenitors via dampening of ROS-induced p53 activity. Cell Stem Cell. 2010;7(5):606-617.

41. Anthony BA, Link DC. Regulation of hematopoietic stem cells by bone marrow stromal cells. Trends Immunol. 2014;35(1):32-37.

42. Challen GA, Sun D, Jeong M, et al. Dnmt3a is essential for hematopoietic stem cell differentiation. Nat Genet. 2011;44(1):23-31.

43. Challen GA, Sun D, Mayle A, et al. Dnmt3a and Dnmt3b have overlapping and distinct functions in hematopoietic stem cells. Cell Stem Cell. 2014;15(3):350-364.

44. Young JH, Logan BR, Wu J, et al. Infections after Transplantation of Bone Marrow or Peripheral Blood Stem Cells from Unrelated Donors. Biol Blood Marrow Transplant. 2016;22(2):359-370.

45. Safdar A, Armstrong D. Infections in patients with hematologic neoplasms and hematopoietic stem cell transplantation: neutropenia, humoral, and splenic defects. Clin Infect Dis. 2011;53(8):798-806.

46. Orazi A, Kahsai M, John K, Neiman RS. p53 overexpression in myeloid leukemic disorders is associated with increased apoptosis of hematopoietic marrow cells and ineffective hematopoiesis. Mod Pathol. 1996;9(1):48-52.

47. Tang F, Barbacioru C, Nordman E, et al. RNA-Seq analysis to capture the transcriptome landscape of a single cell. Nat Protoc. 2010;5(3):516-535.

48. Kim D, Langmead B, Salzberg SL. HISAT: a fast spliced aligner with low memory requirements. Nat Methods. 2015;12(4):357-360.

49. Liao Y, Smyth GK, Shi W. featureCounts: an efficient general purpose program for assigning sequence reads to genomic features. Bioinformatics. 2014;30(7):923-930.

50. Love MI, Huber W, Anders S. Moderated estimation of fold change and dispersion for RNA-seq data with DESeq2. Genome Biol. 2014;15(12):550.

51. Subramanian A, Tamayo P, Mootha VK, et al. Gene set enrichment analysis: a knowledge-based approach for interpreting genome-wide expression profiles. Proc Natl Acad Sci U S A. 2005;102(43):15545-15550.

Conflict of Interest Disclosures

The authors declare no competing financial interests.

Figures and Figure legends

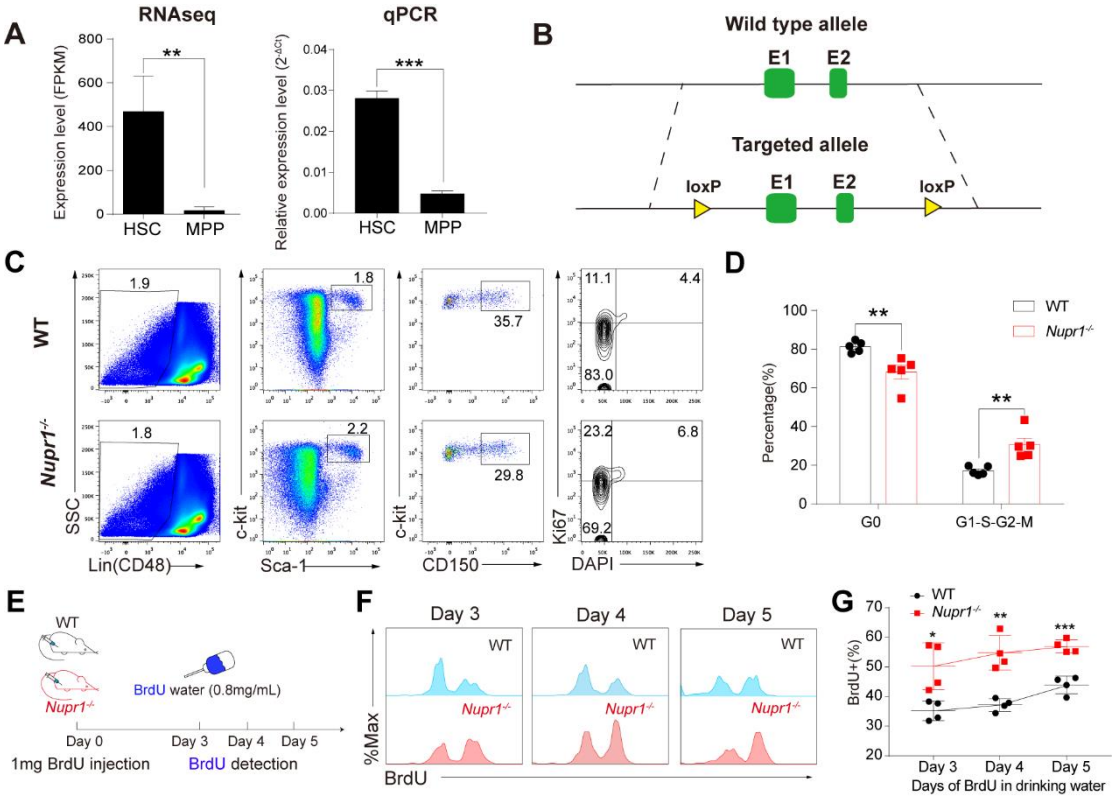

Fig 1. Loss of *Nupr1* activates dormant HSCs under homeostasis

(A) Expression pattern of *Nupr1* in hematopoietic stem cells (HSCs) and multipotent progenitors (MPPs) examined by RNA-sequencing and Real-Time PCR. One thousand HSC or MPP cells from bone marrow of wild type mice were sorted as individual samples for RNA-sequencing (n=4). HSCs are defined as Lin (CD2, CD3, CD4, CD8, Mac1, Gr1, Ter119, B220)$^{-}$, CD48^{-}, Sca1^{+}, c-kit^{+}, and CD150^{+}. MPPs are defined as Lin (CD2, CD3, CD4, CD8, Mac1, Gr1, Ter119, B220)$^{-}$, CD48^{-}, Sca1^{+}, c-kit^{+}, and CD150^{-}. Data are analyzed by unpaired Student's t-test (two-tailed). **p < 0.01, ***p<0.001. Data are represented as mean ± SD (qPCR, n = 3 mice for each group).

(B) Targeting strategy of knockout of *Nupr1* gene in mouse. Wild type *Nupr1* exons 1,

and 2 are shown as green boxes. Two loxp elements flanking exon 1 and exon 2 were inserted.

(C) Cell cycle analysis of *Nupr1*$^{-/-}$ HSCs under homeostasis. Representative plots of cell cycle from representative WT and *Nupr1*$^{-/-}$ mice (8-week-old). WT littermates (8-week-old) were used as control. HSCs (Lin$^-$ (CD2$^-$ CD3$^-$ CD4$^-$ CD8$^-$ B220$^-$ Gr1$^-$ CD11b$^-$ Ter119$^-$) CD48$^-$ Sca1$^+$ c-kit$^+$ CD150$^+$) were analyzed by DNA content (DAPI) versus Ki-67. G0 (Ki-67^{low}DAPI^{2N}), G1 (Ki-67^{high}DAPI^{2N}), G2-S-M (Ki-67^{high}DAPI$^{>2N-4N}$).

(D) Statistical analysis of HSC cell cycle. The percentages (%) of HSCs in G0, G1-G2-S-M stages were analyzed. Data are analyzed by unpaired Student's t-test (two-tailed). **p < 0.01. Data are represented as mean ± SD (n = 5 mice for each group).

(E) The strategy of BrdU incorporation assay. The 8-week-old *Nupr1*$^{-/-}$ mice and littermates were injected intraperitoneally with 1mg BrdU on day 0. Then the mice were continuously fed with BrdU (0.8mg/ml) water until analyzed on day 3, 4, and 5.

(F) Dynamic tendency analysis of BrdU$^+$ HSCs after BrdU administration by flow cytometry on day 3, 4, and 5.

(G) Ratio kinetics of BrdU$^+$ HSCs. Data are analyzed by unpaired Student's t-test (two-tailed). *p < 0.05, **p < 0.01, ***p < 0.001. Data are represented as mean ± SD (n = 4 mice for each group).

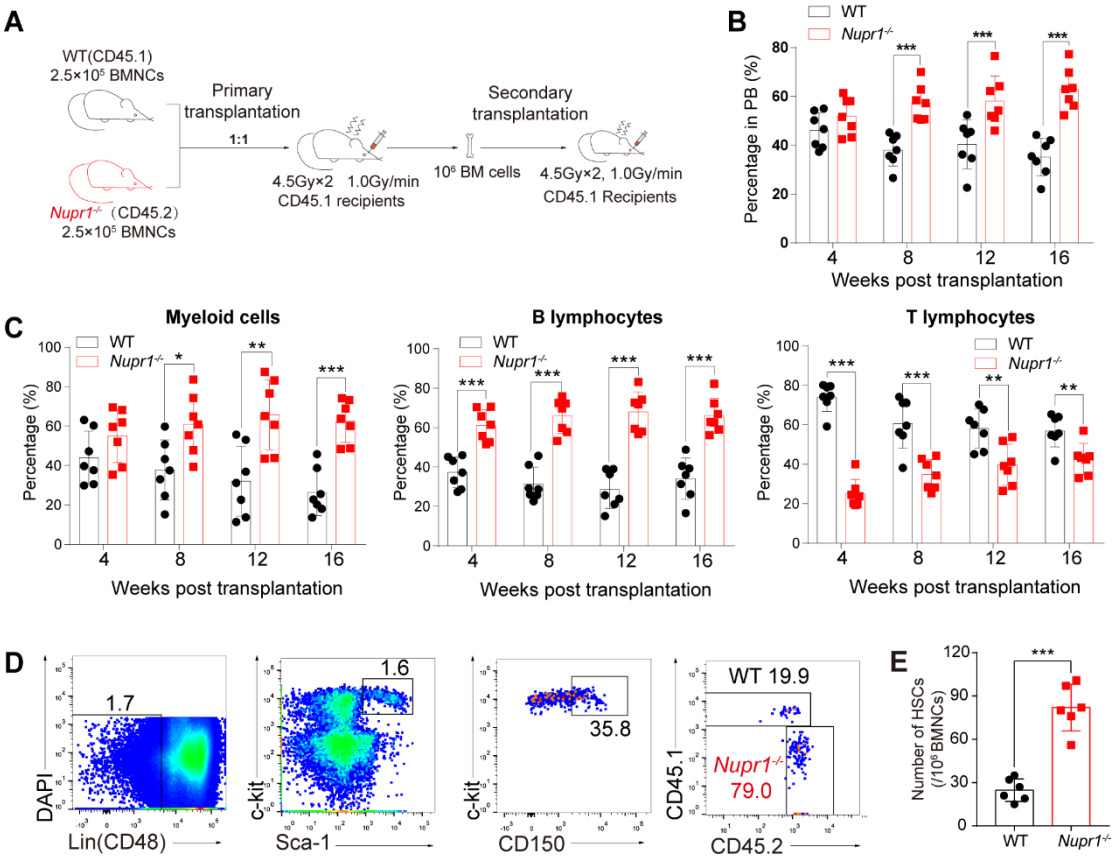

Fig 2. *Nupr1*$^{-/-}$ HSCs show repopulating advantage in competitive transplantation

(A) Schematic diagram of competitive transplantation assay. 2.5×10^5 *Nupr1*$^{-/-}$ BMNCs (CD45.2) and equivalent WT (CD45.1) counterparts were mixed and injected into individual lethally irradiated recipients (CD45.1). Four months later, the recipients were sacrificed. One million BMNCs from primary transplanted recipients were transplanted to lethally irradiated secondary recipients.

(B) Kinetic analysis of donor chimerism ($CD45.2^+$) in peripheral blood. Data are analyzed by paired Student's t-test (two-tailed). ***$p < 0.001$. Data are represented as mean ± SD (n = 7 mice).

(C) Kinetic analysis of of donor-derived lineage chimerism in peripheral blood, including myeloid cells ($CD11b^+$) (left), B lymphocytes ($CD19^+$) (middle), and T

lymphocytes ($CD90.2^+$) (right) in peripheral blood. Data are analyzed by paired Student's t-test (two-tailed). *p < 0.05, **p < 0.01, ***p < 0.001. Data are represented as mean ± SD (n = 7 mice).

(D) Flow cytometry analysis of HSC compartment in primary recipients four months after transplantation. Representative plots from one recipient mouse are shown.

(E) Cell number of donor-derived HSCs in primary recipients four months after competitive transplantation. Data are analyzed by paired Student's t-test (two-tailed). ***p < 0.001. Data are represented as mean ± SD (n = 6 mice).

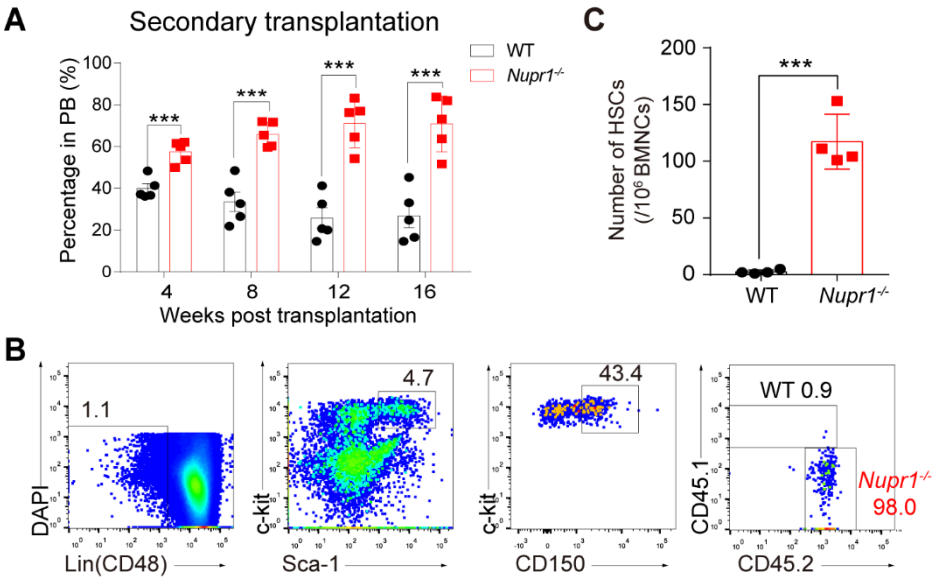

Fig 3. *Nupr1*$^{-/-}$ HSCs continuously show competitive advantage without losing their long-term self-renew ability in secondary transplantation

(A) Kinetic analysis of donor chimerism (CD45.2^{+}) in peripheral blood of secondary transplanted recipients. Data are analyzed by paired Student's t-test (two-tailed). ***p < 0.001. Data are represented as mean ± SD (n = 5 mice).

(B) Flow cytometry analysis of donor *Nupr1*$^{-/-}$ HSCs in secondary recipients four months after transplantation. Representative plots from each group mice were shown.

(C) Cell number of donor-derived HSCs in secondary recipients four months after competitive transplantation. Data are analyzed by paired Student's t-test (two-tailed). ***p < 0.001. Data are represented as mean ± SD (n= 4 mice).

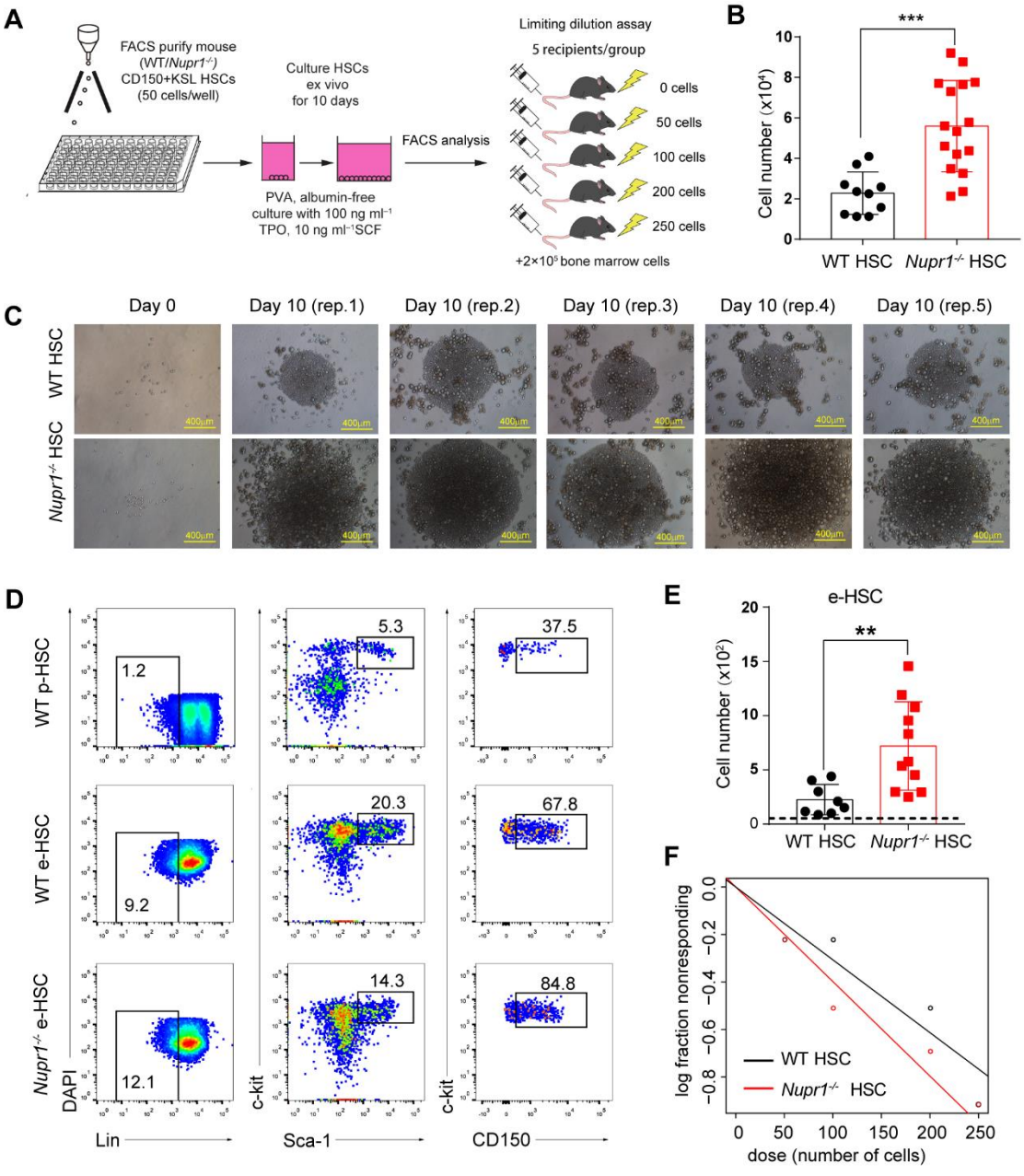

Fig 4. Deletion of *Nupr1* promotes HSC expansion in vitro

(A) Schematic diagram of the HSC expansion in vitro. 50 $CD150^{+}$KSL HSCs (from WT and *Nupr1*$^{-/-}$ mice) were sorted into fibronectin-coated plate wells, containing albumin-free F12 medium supplemented with 1 mg/ml PVA, 100 ng/ml TPO and 10 ng/ml SCF. HSCs were cultured for 10 days and then analyzed by flow cytometry. For limiting dilution assay, serial doses were transplanted into lethally irradiated

563 recipients, together with 2×10^5 bone-marrow competitor cells.

564 (B) Cell number derived from 50 HSCs after a 10-day-long culture in *vitro*. Data are
565 analyzed by unpaired Student's t-test (two-tailed). ***p < 0.001. Data are represented
566 as mean ± SD (WT, n = 10; *Nupr1*$^{-/-}$, n=16)

567 (C) Representative images of WT and *Nupr1*$^{-/-}$ HSCs from freshly isolated HSCs
568 (Day 0) and 10-day-long cultures (Day 10). Images of five representative colonies
569 (biological replicates) are shown.

570 (D) Representative plots of HSC analysis by flow cytometry from cultured WT and
571 *Nupr1*$^{-/-}$ HSCs at day 10. p-HSC indicates primary HSCs from BM. e-HSC indicates
572 expanded HSCs after 10-day culture *ex vivo*.

573 (E) Cell counts of phenotypic CD150^{+}KSL HSCs at day 10 after culture. The dashed
574 indicates the primary input cell amount. Data are analyzed by unpaired Student's t-test
575 (two-tailed). **p < 0.01. Data are represented as mean ± SD (WT, n = 8; *Nupr1*$^{-/-}$,
576 n=11).

577 (F) Poisson statistical analysis after limiting-dilution analysis; plots were obtained to
578 allow estimation of CRU content within each condition (n = 5 mice transplanted at
579 each dose per condition, total 40 mice). The plot shows the percentage of recipient
580 mice containing less than 1% CD45.2^{+} cells in the peripheral blood at 16 weeks after
581 transplantation versus the number of cells injected per mouse.

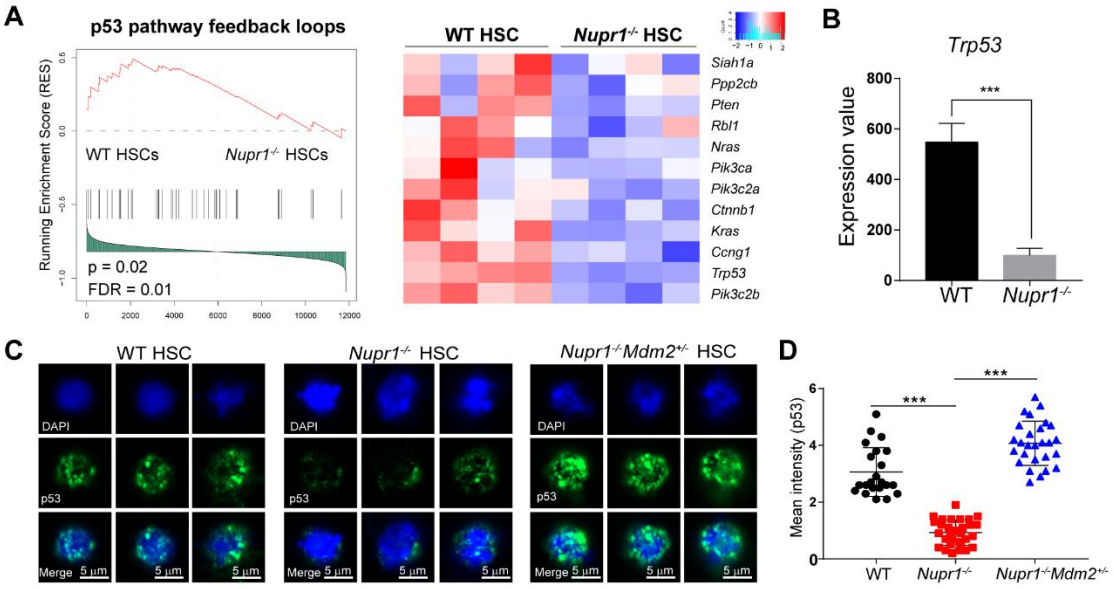

Fig 5. Loss of *Nupr1* confers repopulating advantage on HSCs by regulating p53 check-point signaling

(A) Gene set enrichment analysis (GSEA) of p53 pathway feedback loops in WT HSCs and *Nupr1*$^{-/-}$ HSCs. One thousand HSCs from bone marrow of wild type and *Nupr1*$^{-/-}$ mice were sorted as individual samples for RNA-sequencing. DESeq2 normalized values of the expression data were used for GSEA analysis. Expression of the leading-edge gene subsets was shown. p53 pathway feedback loops-related genes down-regulated in *Nupr1*$^{-/-}$ HSCs (a difference in expression over 1.2-fold; adjusted p value, < 0.05 (DESeq2 R package)). WT HSCs, n = 4 cell sample replicates (one per column); *Nupr1*$^{-/-}$ HSCs, n = 4 cell sample replicates (one per column).

(B) Expression level of p*53* in WT HSCs and *Nupr1*$^{-/-}$ HSCs by RNA-seq. Y-axis indicates the expression value (DESeq2 normalized values of the expression data). The expression value (DESeq2 normalized counts) of each gene was illustrated by graphpad. Data are analyzed by unpaired Student's t-test (two-tailed). ***p < 0.001. Data are represented as mean ± SD (n = 4 mice for each group).

598 (C) Immunofluorescence measurement of p53 proteins in single HSCs from the WT,
599 *Nupr1*$^{-/-}$, *Mdm2*$^{+/-}$*Nupr1*$^{-/-}$ mice. Images of three representative single cell of each
600 group are shown.

601 (D) Mean intensity of p53 fluorescence in WT, *Nupr1*$^{-/-}$, *Mdm2*$^{+/-}$*Nupr1*$^{-/-}$ HSCs. Each
602 dot represents a single cell. Data are analyzed by One-way ANOVA. ***p<0.001.WT,
603 n=22; *Nupr1*$^{-/-}$, n=30; *Mdm2*$^{+/-}$*Nupr1*$^{-/-}$, n=27. Data are represented as mean ± SD.

604

605

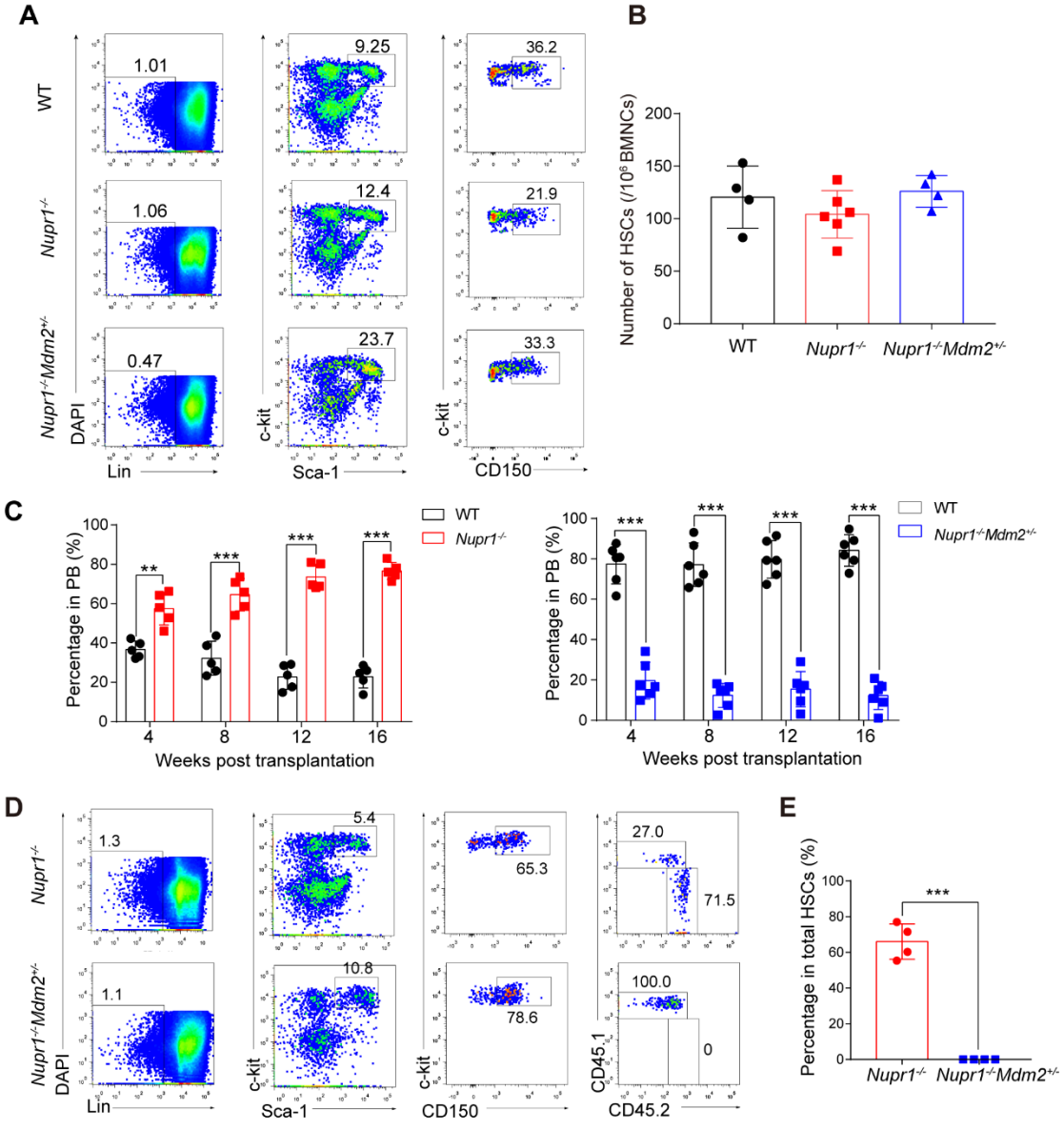

Fig 6. Reversion of p53 expression by allelic depletion of Mdm2 gene offsets the repopulating advantage of *Nupr1*$^{-/-}$ HSCs.

(A) Representative plots of HSC analysis by flow cytometry from WT, *Nupr1*$^{-/-}$ *and* *Nupr1*$^{-/-}$*Mdm2*$^{+/-}$mice bone marrow.

(B) Statistical analysis of WT, *Nupr1*$^{-/-}$ *and Nupr1*$^{-/-}$*Mdm2*$^{+/-}$ HSC number. Data are analyzed by One-way ANOVA. p>0.05. WT, n=4; *Nupr1*$^{-/-}$, n=6; *Mdm2*$^{+/-}$*Nupr1*$^{-/-}$, n=4.

615 (C) Donor bone marrow cells (2.5×10^5) from *Nupr1*$^{-/-}$ (left) or *Nupr1*$^{-/-}$*Mdm2*$^{+/-}$ (right)
616 mice (CD45.2) were transplanted into lethally irradiated recipient mice (CD45.1)
617 along with 2.5×10^5 recipient bone marrow cells. Data are analyzed by paired
618 Student's t-test (two-tailed). **p < 0.01, ***p < 0.001. Data are represented as mean ±
619 SD. *Nupr1*$^{-/-}$, n = 5 mice, *Nupr1*$^{-/-}$*Mdm2*$^{+/-}$, n = 6 mice).
620 (D) Flow cytometry analysis of donor-derived HSCs and recipient HSCs in bone
621 marrow of recipient mice at four months after transplantation. HSCs were gated as
622 CD2$^-$CD3$^-$CD4$^-$CD8$^-$B220$^-$Gr1$^-$Mac1$^-$Ter119$^-$(Lin-) CD48$^-$Sca1$^+$c-Kit$^+$CD150$^+$. Plots
623 from one representative mice of each group are shown.
624 (E) Statistical analysis of donor-derived HSC percentage in recipient mice at four
625 months after transplantation. Data are analyzed by unpaired Student's t-test
626 (two-tailed). ***p < 0.001. Data are represented as mean ± SD (n = 4 mice for each
627 group).
628